1-1-2013

Coarse-Grid Simulations Using Parcels: An Advanced Drag Model based on Filtered CFD-DEM Data

Stefan Radl
Graz University of Technology, Austria

Sankaran Sundaresan
Princeton University, USA

COARSE-GRID SIMULATIONS USING PARCELS:
An Advanced Drag Model based on Filtered CFD-DEM Data

Stefan Radl,[a] and Sankaran Sundaresan[b]

[a]Graz University of Technology; Institute for Process and Particle Engineering, Inffeldgasse 13/III, 8010 Graz, Austria, T: 43-316-873-30412, E: radl@tugraz.at
[b]Dept. of Chemical and Biological Engineering, Princeton University, 08544 Princeton, NJ, T: 1-609-258-4583; E: sundar@princeton.edu

ABSTRACT

We have performed simulations of a freely sedimenting gas-particle suspension to generate data on effective drag coefficients for Euler-Lagrange simulations. We present a model for this effective drag coefficient, and show that this model is able to predict the effective slip velocity within ca. 8% when using extremely coarse computational grids and a parcel approach.

INTRODUCTION

Sedimenting gas-particle mixtures spontaneously form meso-scale structures, i.e., clusters and bubbles, which dramatically change the effective slip velocity between the two phases. Typically, these "meso-scale" structures cannot be resolved when simulating large-scale equipment, and hence one needs to model their effect, e.g., with a model for an effective drag coefficient. Here we refer to simulations that cannot resolve the particle clustering as "coarse-grid" simulations. While numerous models for the effective drag coefficient have been postulated within the last ten years, only few of them have been rigorously validated, or based on detailed simulation data of meso-scale structures. Most of the models have been developed for Two-Fluid-Models (TFM, (1)), and there is now a broad consensus on the structure and benefits of coarse-grid drag models for the TFM (2–5).

For Euler-Lagrange-based (EL) simulations, i.e., for simulations where individual particles or packages thereof ("parcels") are tracked, the question on how to model the drag in coarse-grid simulations has not been answered in sufficient detail. Recent work by Benyahia and Sundaresan (6) indicates that an effective drag model is necessary for EL simulations. The work of Helland and co-workers (7,8), as well as Li et al. (9) have employed an ad-hoc modification of the drag law, or used a drag law designed for TFM-based simulations in EL (coarse-grid) simulations. However, an effective drag law for EL-based, coarse grid simulations with a foundation on detailed simulation data is still missing. Such data can be obtained from (i) fully-resolved direct numerical simulations (DNS, (10)), or (ii) well-resolved EL simulations based on the "CFD-DEM" approach (11,12). Our work is an attempt to develop such an advanced EL-based drag model based on the CFD-DEM approach. This advanced drag model can then be used for coarse-grid simulations using the CFD-DEM approach, as well as coarse-grid CFD-DPM simulations where only packages of particles (but not individual particles) are tracked.

NUMERICAL METHODS AND PARAMETERS

We combine a solver for the incompressible Navier-Stokes equation (to model fluid flow, this solver is based on OpenFOAM 1.7.1) with a high-performance implementation of the discrete element method (DEM; "soft-sphere" approach) on graphic processing units to model the particles.

a) Governing Equations - Fluid Flow

We solve for a spatially-averaged fluid velocity and pressure by using an appropriate mass and momentum balance:

$$\frac{\partial\left(\rho_f \phi_f\right)}{\partial t} + \nabla \cdot \left(\rho_f \phi_f \mathbf{u}\right) = 0 \tag{1}$$

$$\frac{\partial\left(\rho_f \phi_f \mathbf{u}\right)}{\partial t} + \nabla \cdot \left(\rho_f \phi_f \mathbf{u}\mathbf{u}\right) = -\phi_f \nabla p_f - \phi_f \nabla \cdot \boldsymbol{\tau}_f + \boldsymbol{\Phi}_d + \rho_f \phi_f \mathbf{g} \tag{2}$$

Here Φ_d is a volumetric coupling force term (excluding buoyancy effects), i.e. the force exerted by the particle phase on the fluid phase per unit volume of the gas-particle mixture. For modeling Φ_d, we assume that the fluid-particle drag force is the most significant coupling force. Specifically, we use the drag closure of Wen and Yu (13), as well as Beetstra et al. (14). We do not consider pseudo-turbulent motion in the fluid, and employ a simple closure for the fluid stress tensor τ_f based on the molecular viscosity μ_f of the fluid. More details on our solver can be found in our previous publication (15).

b) Governing Equations - Particle Motion

The particle phase is modeled as an assembly of frictional, inelastic spheres, interacting with each other through a linear spring-dashpot model with frictional slider ("soft sphere approach"). Newton's equation of translational and rotational motion is solved. While the latter involves only the torque due to the particle interaction forces, the former yields the following acceleration equation:

$$\mathbf{a} = \frac{\mathbf{f}_{cont,i}}{\rho_p V_{p,i}} + \frac{\beta_{p,i}}{\rho_p}\left(\mathbf{u}_i - \mathbf{v}_i\right) - \frac{1}{\rho_p}\nabla p_{f,i} + \mathbf{g}\,. \tag{3}$$

c) Filtering Strategy

After the flow has reached a statistical steady state, filtering was performed by calculating a Favre-averaged fluid velocity in a filter region with size Δ_{filter}, as well as a corresponding filtered slip velocity:

$$\overline{\mathbf{u}}_{slip,i} = \left(\frac{\overline{\mathbf{u}\,\phi_f}}{\overline{\phi_f}}\right)_i - \mathbf{v}_i\,, \tag{4}$$

A filtered drag coefficient on a "per particle" basis (i indicates the particle index) has been calculated in the vertical direction (indicated by subscript y):

$$\overline{\beta}_{p,i,y} = \frac{1}{\overline{\mathbf{u}}_{slip,i,y}} \left[-\nabla p_{f,i} + \nabla \overline{p}_{f,i} + \beta_{p,i} \left(\mathbf{u}_i - \mathbf{v}_i \right) \right]_y \quad (5)$$

Note that the filtered slip velocity is based on a filtered fluid velocity, and the original (i.e., unfiltered) particle velocity. Samples were collected over a time span of at least $t_{sample} = 30 \cdot u_t / g$ in order to gather a statistical meaningful data.

d) Simulation Parameters

We consider particles with a diameter of d_p = 75 [μm] in a periodic 3-D domain with a width and depth of 106 d_p, as well as a height of 426 d_p. Other parameters (particle properties, grid resolution, etc.) are summarized in Table 1, and symbols are explained in the "Notation" section. The spring stiffness in the DEM interaction model has been selected based on a sufficiently small dimensionless shear rate γ^* to mimic extremely stiff real-world particles. Domain-averaged particle volume fractions $<\phi_p>$ between 0.02 and 0.40 have been considered to construct the filtered drag model.

Parameter	***Value***
ρ_f ; ρ_p	1.3; 1500 [kg/m³]
μ_{pp} ; e_p	0.1 ; 0.9
γ^* ; t^* ; Co ; Δ_{fluid} / d_p	10^{-3} ; 1/50 ; 0.3 ; 3.33
k_n / k_t ; γ_n / γ_t	7/2 ; 1
μ_f	$1.8 \cdot 10^{-5}$ [Pa·s]
G	9.81 [m/s²]
u_t	0.219 [m/s]
Re_p	1.18
Fr_p	65
L_{ref}	$4.86 \cdot 10^{-3}$ [m]

Table 1. Physical properties of the system used to construct the filtered drag model.

RESULTS

a) Filtered Drag Model for Coarse-Grid CFD-DEM Simulations

Based on filtered drag coefficients obtained in various domain-averaged particle volume fractions, we have constructed a model for a filtered drag coefficient of the form (the functions f and h will be published in a future article):

$$\frac{\bar{\beta}_p}{\beta_{p,micro}} = 1 - f\left(F_{f,II}, \bar{\phi}_p\right) h\left(\bar{\phi}_p\right) \tag{6}$$

$$F_{f,II} = \frac{L_{char,II}}{\Delta_{filter}} \tag{7}$$

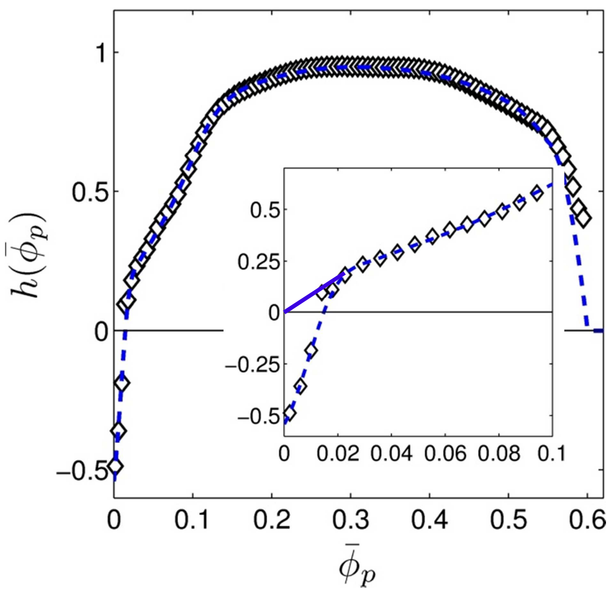

Figure 1. Master curve for h (i.e., the maximum correction to the drag coefficient) as a function of the filtered particle volume fraction (symbols: data from CFD-DEM simulation; dashed line: CFD-DEM data fit; solid line in the insert: low-ϕ_p approximation).

Based on a set of simulations with different particle Froude numbers $Fr_p = u_t^2/d_p g$, we suggest the characteristic length scale

$$L_{char,II} = \frac{u_t^2}{g} Fr_p^{-2/3}$$

as the reference length to scale the filter size Δ_{filter}. The paper of Sundaresan et al., *Coarse-Grained Models for Momentum, Energy and Species Transport in Gas-Particle Flows*, in the proceedings of this conference provides more motivation for this choice.

Our filtered drag model is constituted with $\phi_{p,crit}$ = 0.016, and two master curves for the functions f and h. The latter are functions of the filtered particle volume fraction $\overline{\phi_p}$, and one can fit them to the filtered data using a cubic spline (see Figure 1). The function h represents the maximum correction to the drag coefficient for very large filter sizes. This correction is positive for medium to dense flows (i.e., drag decreases), and negative for very small particle volume fractions (i.e., drag would increase; see the dashed line in Figure 1 that represents our CFD-DEM data). The negative correction results from our definition of the filtered slip velocity, and the fact that particles in relatively dilute regions are strongly accelerated into the positive vertical direction. However, this is a rather unimportant correction for fluidized bed applications, and does not affect the results of coarse-grid simulations of FBs. Hence, we suggest using an extrapolation to $h = 0$ at $\phi_p = 0$ (see the solid line in the insert of Figure 1).

b) Modification for Coarse-Grid CFD-DPM Simulations

Using coarse fluid grids in CFD-DEM simulations results in relatively small savings for the computation time. A concept to further reduce the computational effort is to use so-called "parcel-based" simulations, i.e., to track a small number of surrogate particles that represent a large number of physical particles. Specifically, we use the concept of Patankar and Joseph (16) with appropriately scaled parcel interaction parameters. Parcels are characterized by their relative size α, i.e., the ratio of the (effective) parcel diameter d_{parcel} to the primary diameter d_{prim}. In short, while gas-particle interactions are based on d_{prim}, collision tracking uses d_{parcel}.

It is clear that when using parcels instead of particles, the effect of clustering of the particles that are represented by a single parcel, cannot be taken into account. Thus, even in case we account for the effect of the fluid grid size when using the effective drag coefficient detailed in paragraph a), we will still miss a contribution from the clustering of particles represented by parcels. Here we postulate a simple modification to the effective drag law to account for this effect:

$$\frac{\overline{\beta}_p}{\beta_{p,micro}} = c_{corr}(\alpha)\left[1 - f\left(F_{f,II}, \overline{\phi}_p\right) h\left(\overline{\phi}_p\right)\right], \tag{8}$$

We close this model with:

$$c_{corr} = a + (1-a)\exp\left[-k\left(\alpha - 1\right)\right] \tag{9}$$

with the parameters $a = 0$, and $k = 0.05$. The latter coefficient is based on fits to coarse-grid CFD-DPM simulation data. The rationale behind setting $a = 0$ is that we were unable to run simulations with $\alpha > 8$ in the relatively small domain that we considered. For very large parcels, more simulations in larger boxes would be required to find more accurate values for a and k.

c) Coarse-Grid CFD-DEM and CFD-DPM

We now demonstrate that our model is indeed able to correctly predict the time-averaged sedimentation velocity when performing coarse-grid simulations. In Figure 2 we display results of CFD-DEM simulations using various grid resolutions (all particles are tracked in these simulations). Clearly, using a microscopic drag law (as indicated by "Beetstra" in Figure 2) yields a grid-dependent slip velocity (here $\mathbf{u}_{slip,y}$ indicates the domain-averaged slip velocity in the direction parallel to gravity). Instead, using a filtered drag model (i.e., the one displayed in Eqn. 6) yields results much closer to well-resolved CFD-DEM simulations, even on extremely coarse grids.

Finally, we show that our model is able to predict the effective slip velocity reasonably well when using extremely coarse computational grids and tracking only a small number of computational parcels (see Figure 3).

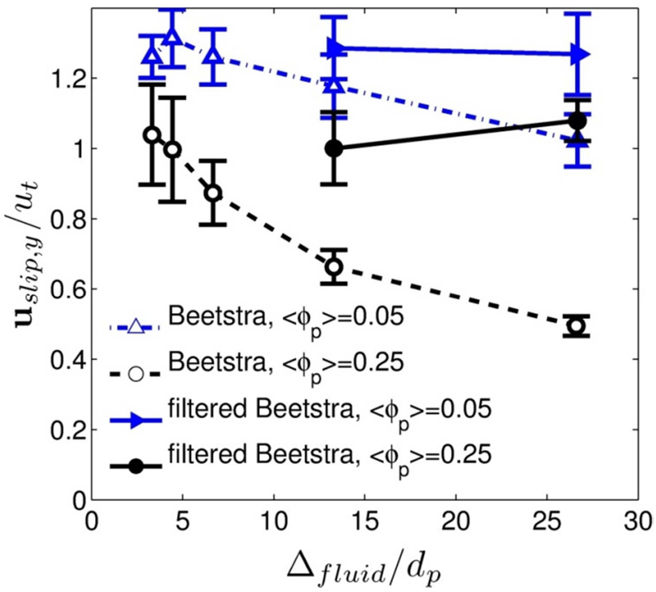

Figure 2. Normalized domain-averaged slip velocity for CFD-DEM-based simulations (open symbols; the errorbars indicate the standard deviation of the slip velocity over time; Beetstra et al.'s drag law without modification) and coarse-grid CFD-DEM-based simulation using an effective drag model (filled symbols; modified Beetstra et al. drag model).

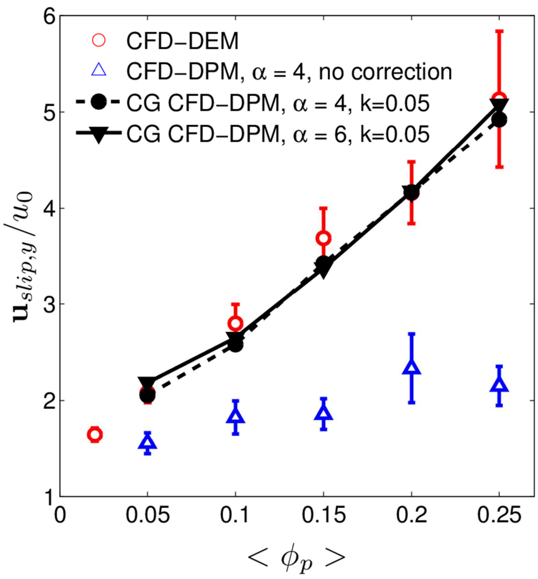

Figure 3. Normalized domain-averaged slip velocity for CFD-DPM-based simulations (the red symbols indicate resolved CFD-DEM data with error bars indicating the standard deviation; blue and black symbols represent CFD-DPM simulations with or without the filtered drag model given by Eqn. 8; Δ_{fluid}/d_{prim} = 26).

As can be seen, the filtered drag model predicts the slip velocity within the standard deviation of the CFD-DEM results even when tracking only $1/6^3$ = 1/216th of the particles (see results for α = 6 in Figure 3). In these simulations the fluid grid resolution is approximately 8 times larger than the one required for well-resolved CFD-DEM-base simulations.

ACKNOWLEDGMENT

SR acknowledges support through Project J-3072 sponsored by the Austrian Science Foundation.

NOTATION

Latin Symbols

Co	(maximum) Courant number for fluid flow
$Fr_p = u_t^2 / \left(g\, d_p\right)$	particle Froude number
$L_{char,II}$	(cluster) characteristic length [m]
V_p	particle volume [m³]
a	parameter (parcel size correction function)
$a_{Ff,II}$	filtered drag correction function
c_{corr}	parcel size correction function
d_p	particle diameter [m]
$e_p = \exp\left(-\gamma_n \pi / \sqrt{4k_n / \left(m_{12} - \gamma_n^2\right)}\right)$	coefficient of restitution
$\mathbf{f}_{cont}$	contact force [N]
f	filtered drag correction function
g	gravitational acceleration [m/s²]
h	filtered drag correction function
k	parameter (parcel size correction function)
k_n ; k_t	spring stiffness (normal/tangential) [N/m]
$m_{12} = m_1 m_2 / (m_1 + m_2)$	reduced mass [kg]
p_f	(fluid) pressure [Pa]
$t_c = \pi / \sqrt{k_n / m_{12} - \gamma_n^2 / \left(2m_{12}\right)^2}$	characteristic contact time [s]
$t^* = \Delta t / t_c$	dimensionless time step
u_t	terminal settling velocity [m/s]

Greek Symbols

Φ_d	volumetric coupling force [N/m³]
α	dimensionless parcel size
β_p	(microscopic) drag coefficient [kg/s/m³]
Δ_{fluid}	fluid grid resolution [m]
Δ_{filter}	filter size [m]
γ_n; γ_t	damping coefficient (normal/tangential) [Ns/m]
$\gamma^* = \left(u_t\, d_p / g\right) / \sqrt{k_n / \left(d_p\, \rho_p\right)}$	dimensionless shear rate
ϕ_p, ϕ_f	particle volume fraction, void fraction
μ_{pp}	particle-particle friction coefficient
μ_f	dynamic viscosity [Pa·s]
ρ_p ; ρ_f	density (particle/fluid) [kg/m³]

REFERENCES

1 T.B. Anderson and R. Jackson, A Fluid Mechanical Description of Fluidized Beds. I&EC Fundamentals 6 (1967) 527–539.

2 J. Wang, M. a. van der Hoef, and J. a. M. Kuipers, Coarse grid simulation of bed expansion characteristics of industrial-scale gas–solid bubbling fluidized beds. Chemical Engineering Science 65 (2010) 2125–2131.

3 Y. Igci and S. Sundaresan, Constitutive Models for Filtered Two-Fluid Models of Fluidized Gas-Particle Flows. Industrial & Engineering Chemistry Research 50 (2011) 13190–13201.

4 J.-F. Parmentier, O. Simonin, and O. Delsart, A functional subgrid drift velocity model for filtered drag prediction in dense fluidized bed. AIChE Journal 58 (2012) 1084–1098.

5 N. Yang, W. Wang, W. Ge, and J. Li, CFD simulation of concurrent-up gas–solid flow in circulating fluidized beds with structure-dependent drag coefficient. Chemical Engineering Journal 96 (2003) 71–80.

6 S. Benyahia and S. Sundaresan, Do we need sub-grid scale corrections for both continuum and discrete gas-particles flow models? Powder Technology 220 (2012) 2–6.

7 E. Helland, H. Bournot, R. Occelli, and L. Tadrist, Drag reduction and cluster formation in a circulating fluidised bed. Chemical Engineering Science 62 (2007) 148 – 158.

8 E. Helland, R. Occelli, and L. Tadrist, Numerical study of cluster and particle rebound effects in a circulating fluidised bed. Chemical Engineering Science 60 (2005) 27–40.

9 F. Li, F. Song, S. Benyahia, W. Wang, and J. Li, MP-PIC simulation of CFB riser with EMMS-based drag model. Chemical Engineering Science 82 (2012) 104–113.

10 J.J. Derksen and S. Sundaresan, Direct numerical simulations of dense suspensions: wave instabilities in liquid-fluidized beds. Journal of Fluid Mechanics 587 (2007) 303–336.

11 B.P.B. Hoomans, J.A.M. Kuipers, W.J. Briels, and W.P.M. vanSwaaij, Discrete particle simulation of bubble and slug formation in a two-dimensional gas-fluidised bed: A hard-sphere approach. Chemical Engineering Science 51 (1996) 99–118.

12 Z.Y. Zhou, S.B. Kuang, K.W. Chu, and A.B. Yu, Discrete particle simulation of particle–fluid flow: model formulations and their applicability. Journal of Fluid Mechanics 661 (2010) 482–510.

13 C. Wen and Y. Yu, Mechanics of fluidization. Chem. Eng. Prog. Symp. Ser. 62 (1966) 100–111.

14 R. Beetstra, M.A. Van Der Hoef, and J.A.M. Kuipers, Drag Force of Intermediate Reynolds Number Flow Past Mono- and Bidisperse Arrays of Spheres. AIChE Journal 53 (2007) 489–501.

15 S. Radl, M. Girardi, and S. Sundaresan, Effective Drag Law for Parcel-Based Approaches - What Can We Learn from CFD-DEM? in: ECCOMAS 2012, J. Eberhardsteiner, ed. Vienna, Austria: 2012.

16 N.A. Patankar and D.D. Joseph, Modeling and numerical simulation of particulate flows by the Eulerian-Lagrangian approach. International Journal of Multiphase Flow 27 (2001) 1659–1684.